Fluid-Mineral Interactions: A Tribute to H. P. Eugster
© The Geochemical Society, Special Publication No. 2, 1990
Editors: R. J. Spencer and I-Ming Chou

Quantitative redox control and measurement in hydrothermal experiments

I-MING CHOU and GARY L. CYGAN
959 National Center, U.S. Geological Survey, Reston, Virginia 22092, U.S.A.

Abstract—In situ redox measurements have been made in sealed Au capsules containing the assemblage Co-CoO-H_2O by using hydrogen-fugacity sensors at 2 kbar pressure with three different pressure media, Ar, CH_4 and H_2O, and between 500 and 800°C. Results show that equilibrium redox states can be achieved and maintained under Ar or CH_4 external pressure, but they cannot be achieved and maintained at temperatures above 600°C under H_2O external pressure. The conventional assumption that equilibrium redox condition is achieved at a fixed *P-T* condition in the presence of a redox buffer assemblage is therefore not necessarily valid, mainly due to the slow kinetics of the buffer reaction and/or the high rate of hydrogen leakage through the buffer container. The inconsistent equilibrium phase boundaries for the assemblage annite-sanidine-magnetite-fluid reported in the literature can be explained by the inadequate redox control in some of the earlier experiments. The attainment of redox equilibrium in hydrothermal experiments should be confirmed by the inclusion of a hydrogen-fugacity sensor in each experiment where the redox state is either quantitatively or semiquantitatively controlled.

INTRODUCTION

THE PIONEERING WORK OF EUGSTER (1957) on the solid oxygen buffer technique provides a convenient way to control redox states in hydrothermal experiments. Information on the technique's basic theory, the experimental setups of the original design as well as its variations, and its applications are contained in papers by HUEBNER (1971) and CHOU (1987a). The basic experimental assembly consists of two nested capsules (Fig. 1) and has often been referred to as the double-capsule technique. The mineral assemblage under study and water are sealed in the inner capsule, constructed of either Pt or one of the Ag-Pd alloys, which are highly permeable to hydrogen. This charge system, together with an oxygen buffer assemblage and water, is in turn sealed in a larger outer capsule, made of either Au or Ag, which are relatively impermeable to hydrogen. When this assembly is run at a fixed *P-T* condition, the unknown redox state of the charge system is compared with the known redox state of the buffer system by examining the direction of the redox reaction in the charge system after quench.

Suppose that the reversal of the redox reaction of the charge system can be demonstrated at a given pressure P within a minimum temperature bracket $\Delta T = T_2 - T_1$, where $T_2 > T_1$. Then the equilibrium of the redox reaction of the charge system is located at $T = [(T_2 + T_1)/2] \pm (\Delta T/2)$ and at the redox state of the buffer system, assuming that the equilibrium redox states of the buffer system had been achieved and maintained during the run. However, our recent redox measurements of the buffer system by using the hydrogen fugacity sensors (CHOU and EUGSTER, 1976; CHOU, 1978, 1987a,b) indicate that this assumption is not always valid. Therefore, some of the published data on the mineral stability relations in P-T-fO_2 or P-T-fH_2 space obtained by using the oxygen-buffer technique may not be reliable, as indicated, for example, by the recent data on annite (HEWITT and WONES, 1981, 1984). Therefore, we will re-evaluate the oxygen-buffer technique based upon our fH_2-sensor measurements in this paper, point out some potential inherent problems, and provide remedies. Preliminary results have been presented earlier (CHOU and CYGAN, 1987, 1989; CHOU, 1988).

THE EQUILIBRIUM ASSUMPTION OF THE BUFFER SYSTEM

In the application of the oxygen-buffer technique, it is commonly assumed that the redox state of the buffer system at P and T is fixed at the equilibrium condition if the phases of the buffer assemblage (oxygen buffer plus water) are present after the experiment as demonstrated by X-ray and/or optical methods after quench. However, several factors may affect the validity of this equilibrium assumption: (1) a buffer phase may alloy with the container material, thus changing its activity (HUEBNER, 1971); (2) a buffer phase may be isolated by the armoring of the reactant by a layer of buffer reaction product; (3) hydrogen may leak through the external capsule; and (4) the buffer reactions may have slow kinetics.

Alloying of a buffer phase with the container material has been examined by the establishment and maintenance of steady-state hydrogen fluxes through the wall of the inner capsule. The experimental setup is the same as shown in Fig. 1 except that the charge system is replaced by another oxygen

buffer + H_2O assemblage (CHOU, 1986). In relatively short experiments, the alloying is not a significant problem. The decay of the steady-state hydrogen fluxes observed in the same experiments with longer durations (CHOU, 1986, his Fig. 4) is at least partially attributed to the armoring of buffer phases, which prevents equilibrium redox control of the buffer assemblages on both sides of the inner membrane. The existence of the alloying and armoring problems in certain runs may be inferred from inconsistent experimental results but is generally difficult to identify unambiguously. The use of the hydrogen-fugacity sensor technique (CHOU and EUGSTER, 1976; CHOU, 1978, 1987a,b) makes it possible to identify when alloying and amoring significantly affect equilibrium redox conditions and also to identify the problems of hydrogen leakage and slow kinetics. The nature of the last two problems will be presented after a brief review of the fH_2 sensor technique.

THE HYDROGEN-FUGACITY SENSOR TECHNIQUE

A brief summary of the technique is given here. For additional information on the theory, experimental details, and applications, the reader is referred to previous publications (CHOU, 1978, 1987a,b, 1989). To prepare a typical sensor, 10–20 μL of solution, either distilled H_2O (for a type A sensor) or 3 m HCl (for a type B sensor), together with ~20 mg Ag and ~20 mg AgCl are loaded into a Pt or AgPd capsule, 1.85 mm OD, 1.54 mm ID, 19 mm long, which is then welded shut. These sensors are then exposed to a system, whose fH_2 is to be measured at P and T. It has been shown that

$$(fH_2)_{P,T} = (K_1)_{P,T}(m_{HCl})^2_{P,T} \qquad (1)$$

where K_1 is a constant at a fixed P-T condition and $(m_{HCl})_{P,T}$ is the molality of associated HCl at P and T calculated from the total Cl^- molarity measured after quench, $(M_{Cl^-})_{1\ atm,\ 25°C}$ (CHOU, 1987a). The attainment of H_2 osmotic equilibrium in the system is indicated by similar measured values of $(M_{Cl^-})_{1\ atm,\ 25°C}$ in sensors A and B. The $(M_{Cl^-})_{1\ atm,\ 25°C}$ values range from ~0.05 for the magnetite-hematite-H_2O assemblage at 2 kbar and 600°C to ~2.0 for Co-CoO-H_2O assemblage at 2 kbar and 800°C. For more reducing conditions, it is advantageous to use the analogous Ag-AgBr-HBr type of fH_2 sensor instead of the Ag-AgCl-HCl type, since the Br^- concentrations in the sensors are about an order of magnitude lower than those of Cl^- under the same P-T-fH_2 conditions, so that m_{Br^-} can be approximated by M_{Br^-}. To prepare the Ag-AgBr-HBr type of fH_2 sensor, AgCl is replaced by AgBr and 3 m HCl is replaced by 1.5 M HBr in the procedures described above for the preparation of the Ag-AgCl-HCl type. The Ag-AgBr-HBr type of fH_2 sensor has been used to calibrate the graphite-methane buffer (CHOU, 1987b) and monitor the fH_2 in the relatively reducing assemblage WO_2-H_2O (CYGAN and CHOU, 1987) according to the relation

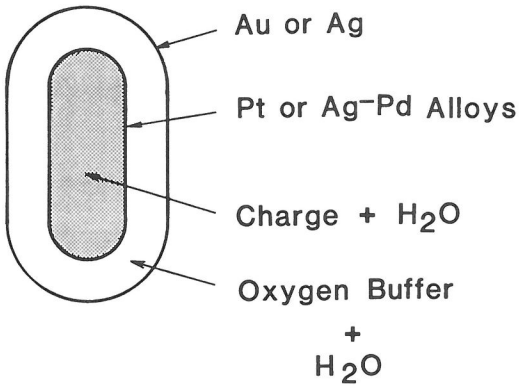

FIG. 1. Schematic diagram showing experimental arrangement of the oxygen buffer technique developed by EUGSTER (1957).

$$(fH_2)_{P,T} = (K_2)_{P,T}(m_{HBr})^2_{P,T}$$
$$\approx (K_2)_{P,T}(M_{Br^-})^2_{1\ atm,\ 25°C} \qquad (2)$$

where K_2 is a constant, $(m_{HBr})_{P,T}$ is molality of associated HBr at P and T, and $(M_{Br^-})_{1\ atm,\ 25°C}$ is molarity of Br^- in the sensor measured after quench. The above approximation relation is only valid when HBr at P and T is mostly associated; otherwise the HBr dissociation constant at P and T is needed to convert $(M_{Br^-})_{1\ atm,\ 25°C}$ to $(m_{HBr})_{P,T}$.

HYDROGEN LEAKAGE AND THE EFFECT OF THE PRESSURE MEDIUM

As mentioned earlier, Au and Ag capsules are commonly used as containers for the buffer assemblage (see Fig. 1) because they are relatively impermeable to hydrogen. However, since these materials are still permeable to hydrogen, especially at temperatures above 650°C (CHOU, 1986, his Fig. 3), it is unavoidable that the choice of the external pressure medium used in the buffer experiments will have some effect on the rate of hydrogen leakage through the wall of external capsule and hence may affect the redox state of the buffer system, especially when the buffer reaction is sluggish. To assess these effects, we performed a series of experiments using the fH_2 sensors to monitor simultaneously the redox states in the buffer system and in three different

pressure media: Ar, CH_4, and H_2O. The effect of the external pressure medium on the fH_2 that can be maintained in a sealed Au capsule containing the buffer assemblage Co-CoO-H_2O was examined at 2 kbar and between 500 and 800°C. The Au capsules used were 0.2 mm thick and 25.4 mm long and had an ID of either 4.0 mm or 2.7 mm. Three different capsule arrangements were used (Fig. 2). In arrangement (a) shown in Fig. 2, fH_2 sensors A and B were exposed to the Co-CoO-H_2O buffer system, and the degree of attainment of osmotic equilibrium can be demonstrated in each run. In arrangement (b), only one fH_2 sensor was exposed to the buffer system in order to save more room for the buffer assemblage; the durations of the runs were longer than those required for the attainment of osmotic equilibrium established by experiments using arrangement (a). Arrangement (c) was similar to (b), except that an extra layer of Au capsule containing the same buffer assemblage was added to minimize the hydrogen gradient and hence hydrogen transfer across the inner Au capsule wall. In all three experimental setups, an additional fH_2 sensor was placed adjacent to the capsule to monitor redox state in the pressure medium. Experiments were performed in Stellite 25* cold-seal pressure vessels using Ar, H_2O, or CH_4 as a pressure medium. The experimental setup was similar to that used to calibrate the C-CH_4 buffer (CHOU, 1987b, his Fig. 1), except that stainless steel instead of graphite filler rods were used when the pressure medium was Ar or H_2O. Both the Ag-AgCl-HCl type and the Ag-AgBr-HBr type of fH_2 sensor were used in this study. The experimental procedures were the same as those described previously (CHOU, 1987b). In addition, the H_2O budget in the Co-CoO-H_2O assemblage was determined for some of the runs in order to monitor the rate of H_2 permeation through the Au capsule wall. According to the reaction

$$Co_{(s)} + H_2O_{(g)} = CoO_{(s)} + H_{2(g)}, \qquad (3)$$

for every mole of H_2 being added to or subtracted from the system, one mole of H_2O is created or consumed, respectively. Therefore, the average permeation rates of hydrogen through the Au capsule can be calculated from the weight change of H_2O in the capsule; the initial weight of H_2O is measured during loading and the final weight of H_2O after quench is measured by the weight-loss method (CHOU, 1986).

Experimental results are given in Table 1 and shown in Figs. 3 and 4. All of the experimental data under CH_4 external pressure shown in Fig. 3 are taken from CHOU (1987b, his Table 1) except one run (no. 28 in Table 1), in which the H_2O budget in the Au capsule was obtained to demonstrate that hydrogen diffuses into instead of out of the Au capsule. Experimental results under Ar pressure medium are also shown in Fig. 3 for comparison. The data are plotted in terms of log M_{Br^-}, which can be related to log fH_2 through Equation (2). Redox states of the pressure medium in some runs are measured by using the Ag-AgCl-HCl sensors, and the results in $(M_{Cl^-})_{1\ atm,\ 25°C}$ are converted to M_{Br^-} through the relation

$$(fH_2)_{P,T} = (K_1)_{P,T}(m_{HCl})^2_{P,T}$$
$$= (K_2)_{P,T}(M_{Br^-})^2_{1\ atm,\ 25°C} \qquad (4)$$

where $(m_{HCl})_{P,T}$ is calculated from $(M_{Cl^-})_{1\ atm,\ 25°C}$

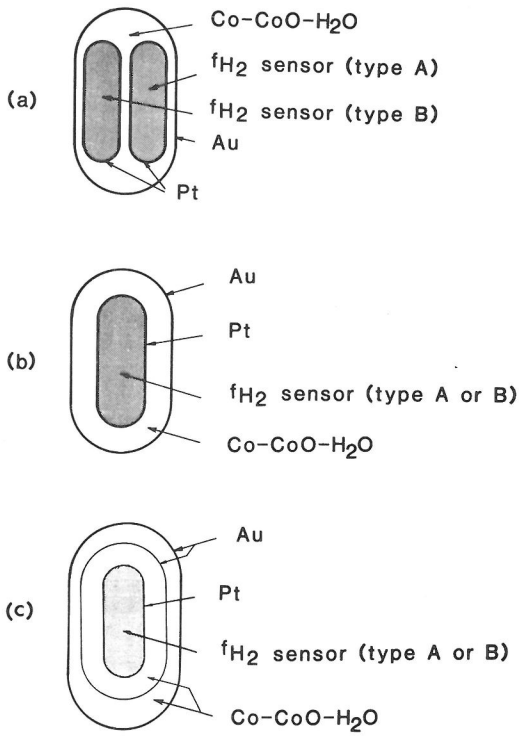

FIG. 2. Schematic diagrams showing three types of experimental arrangements used in this study to measure fH_2 in Au capsules containing the buffer assemblage Co-CoO-H_2O. Type A of fH_2 sensor uses H_2O as a starting solution, and type B uses acid solution (either 3 *m* HCl or 1.5 *M* HBr) as a starting solution (for detail, see text). The capsules were pressurized externally at 2 kbar by Ar, H_2O, or CH_4 and an additional fH_2 sensor (type A or B) was exposed directly to the pressure medium to measure its redox state at *P* and *T*. Results are given in Table 1 and Figs. 3 and 4.

* Registered trademark of Haynes Stellite Co. Use of trade names in this publication is for descriptive purposes only and does not constitute endorsement by the U.S. Geological Survey.

Table 1. Experimental results of the effect of pressure medium on the redox states of the buffer assemblage Co-CoO-H_2O contained in Au capsules of 0.2 mm wall thickness at 2 kbar total pressure

Run no.	Experimental setup[a]	T (°C)	Duration, t (hrs.)	Log M_{Br^-}[b] Co-CoO-H_2O	Log M_{Br^-}[b] Pressure medium	wt. of H_2O (mg)[c] Initial	wt. of H_2O (mg)[c] Final	$\Delta H_2O/t$[d] (μg/hr)
				(A) Ar pressure medium				
23	b	800	8	(−0.800)	−1.043[h]	24.95	22.47	−310.0
21	b	800	8	−0.821	n.d.[e]	24.35	21.66	−336.3
22	b	752	16	−0.852	−1.260[h]	25.28	22.03	−203.1
24A	b	701	52	−0.838	−1.040[h]	23.44	18.19	−101.1
19	b	700	68	(−0.872)	−0.942	26.18	23.05	−46.0
26	a	651	96	−0.876; (−0.911)	−1.190[h]	19.93	15.71	−44.0
27	a	601	120	−0.938; (−0.980)	−1.470[h]	25.23	24.15	−9.0
29	a	550	167	−1.093; (−1.087)	−1.520	19.80	15.91	−23.3
29A	a	550	120	−1.063; (−1.099)	n.d.	20.00	19.51	−4.1
25	a	500	288	−1.121; (−1.102)	−1.180	25.33	24.99	−1.2
				(B) H_2O pressure medium				
11	b	800	20	(−1.137)	n.d.	10.00	5.70	−215.0
12	b	800	19	−1.151	n.d.	n.d.	n.d.	n.d.
15	c	800	6	−1.204	n.d.	n.d.	n.d.	n.d.
18	c	800	10	−1.134	−1.101	16.30	10.21	−609.0
C8	b	800	25	n.l.[f]	−1.000; (−0.988)	n.a.[g]	n.a.	n.a.
2	a	750	49	−1.070; (−1.132)	−1.201	n.d.	n.d.	n.d.
7	c	750	46	−1.135	n.d.	12.45	10.08	−51.5
4	c	706	90	−1.071	n.d.	17.01	n.d.	n.d.
1	a	700	72	−1.174; (−1.180)	−1.359; (−1.348)	39.36	n.d.	n.d.
9	c	700	96	(−1.008)	n.d.	13.29	7.96	−55.5
E	b	700	48	(−1.205)	n.d.	20.95	17.07	−80.8
34	a	696	48	−1.245; (−1.327)	−1.319	20.28	18.09	−45.6
8	c	650	120	−1.117	n.d.	18.22	11.99	−51.9
5	c	600	188	−1.101	n.d.	14.77	9.38	−23.4
10	c	600	23	(−1.025)	n.d.	15.00	n.d.	n.d.
33	a	595	163	−1.148; (−1.161)	−1.581	30.12	27.70	−14.8
14	b	500	240	−1.140	n.d.	20.00	16.71	−13.7
17	b	500	240	(1.160)	−1.343	20.00	19.70	−1.25
				(C) CH_4 pressure medium				
28	a	650	120	−0.895; (−0.908)	−0.768	22.96	25.08	17.7

[a] As shown in Fig. 2.
[b] Numbers in parentheses are from sensors using 1.5M HBr as a starting solution; the rest are from sensors using H_2O as a starting solution. The relation between log M_{Br^-} and log fH_2 can be obtained from Equation (4). Results are shown in Figs. 3 and 4.
[c] Weight of H_2O in Au capsules containing the buffer assemblage Co-CoO-H_2O. For those using double Au capsules (setup (c) in Fig. 2), the numbers given are for the inner Au capsule; the final wt. of H_2O in the outer Au capsule was determined for run no. 18 only. The $\Delta H_2O/t$ for the outer Au capsule in this run was −1143 (μg/hr) including the H_2O loss from the inner Au capsule.
[d] Average rates of H_2O generation (positive) or consumption (negative) in the Au capsules; to obtain rates of H_2 gain or loss, see Equation (5).
[e] Not determined.
[f] Not loaded.
[g] Not applicable.
[h] Calculated from measured m_{Cl^-} using Equation (4).

and the ionization constant of HCl (for detail, see CHOU, 1987a). The data shown in Fig. 3 indicate that equilibrium redox states (shown by the open symbols) can be maintained in the Au capsule for the assemblage Co-CoO-H_2O at 2 kbar CH_4 or Ar external pressure; these redox states are represented by the solid line, which is the least-squares fit of the data.

The reasons for choosing the Co-CoO-H_2O buffer in this study are that the buffer reaction is kinetically fast and that, at P and T, the assemblage defines redox states (open symbols in Fig. 3) that are in-

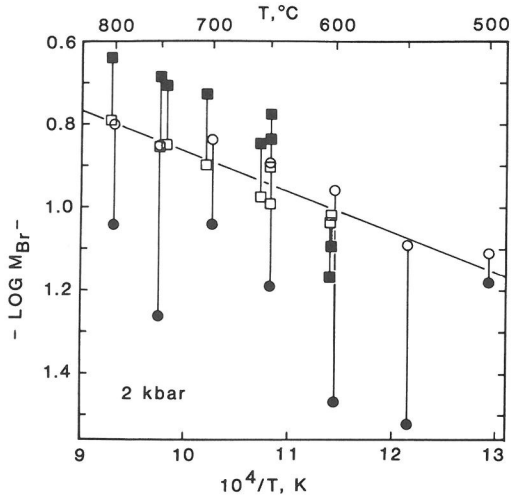

FIG. 3. Experimental results of fH_2-sensor measurements in Au capsules of 0.2 mm wall thickness containing the buffer assemblage Co-CoO-H_2O at 2 kbar Ar (open circles) and CH_4 (open squares) external pressure. The corresponding redox measurements of the pressure medium at P and T in these runs are shown by the filled symbols connected by the vertical lines. The plotted data are given in Table 1 and in CHOU (1987b, his Table 1). For runs containing both sensors A and B (type (a) in Fig. 2), average values are plotted. The solid line with a negative slope is the least-squares fit of all the data shown by the open symbols and can be represented by the equation log $M_{Br^-} = 0.1096 - 974.6/T$, K ($r^2 = 0.8928$). The relationship between fH_2 and M_{Br^-} is given in Equation (2). Equilibrium redox states for the buffer assemblage Co-CoO-H_2O were attained in these experiments in the Au capsules.

termediate between those of the pressure media, with CH_4 being more reducing (filled squares in Fig. 3 at $T \geq 650°C$) and Ar more oxidizing (filled circles in Fig. 3). Reversal of the buffer reaction (Equation 3) can be demonstrated by consideration of the H_2O budget in the system. Under Ar pressure, H_2 diffuses out of the Au capsule and the buffer reaction consumes H_2O, while under CH_4 pressure at $T \geq 650°C$, H_2 diffuses into the Au capsule and generates H_2O. The H_2O budget data are listed in Table 1. Also listed are the average rates of H_2O consumption (negative sign) or generation (positive sign), $\Delta H_2O/t$. The average permeation rates of H_2 through the Au capsules can be calculated from

$$\Delta H_2/t = (\Delta H_2O/t) \times (2.016/18.015) \quad (5)$$

where ΔH_2 and ΔH_2O are weight changes in H_2 and H_2O, respectively, in the buffer system, t is duration of the run, and 2.016 and 18.015 are molecular weights of H_2 and H_2O, respectively. A positive sign indicates influx of H_2 and a negative sign indicates outflow of H_2. The $\Delta H_2O/t$ data given in Table 1 are obtained by ignoring the minor hydrogen exchanges between the fH_2 sensor and the Co-CoO-H_2O system. Also, these average rates of H_2O consumption or generation are not necessarily equivalent to the rates at steady-state conditions; during the run, the redox states of the pressure media and hence the H gradients in the Au membrane are not rigorously defined so the presence or absence of steady-state conditions cannot be determined. Nevertheless, the $\Delta H_2O/t$ data can provide rough estimates on the rates of H_2 transfer as indicated by the rather systematic changes in $\Delta H_2O/t$ under Ar external pressure, which range from -1.2 μg/hr at 500°C to -310 μg/hr at 800°C. The H_2O budget was not determined in the earlier experiments under CH_4 external pressure (CHOU, 1987b); the H_2O budget determined in run no. 28 (listed in Table 1) indicates influx of H_2 with a $\Delta H_2O/t = 1.77$ μg/hr.

Experimental results obtained by using H_2O as a pressure medium are listed in Table 1 and shown in Fig. 4. The data plotted in Fig. 4 show that at temperatures above 600°C, equilibrium redox conditions of the Co-CoO-H_2O assemblage, represented by the solid line derived from Fig. 3, cannot be achieved and maintained in the Au capsules. At these temperatures, the pressure medium exerts a

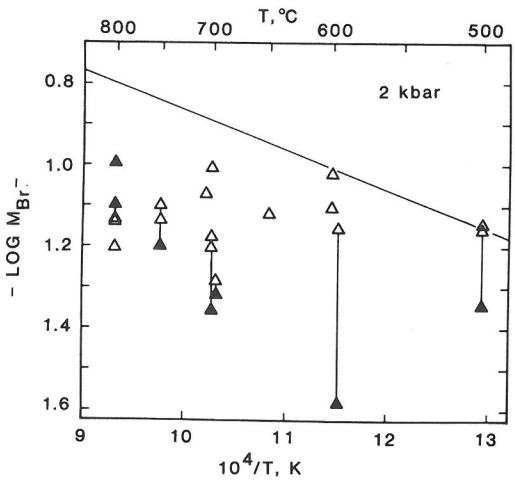

FIG. 4. Experimental results of fH_2-sensor measurements in Au capsules of 0.2 mm wall thickness containing the buffer assemblage Co-CoO-H_2O at 2 kbar H_2O external pressure (open triangles). The filled triangles represent the corresponding redox measurements of the pressure medium. The plotted data are given in Table 1. For runs containing both sensors A and B, average values are plotted. The equilibrium redox states of the Co-CoO-H_2O buffer is shown by the solid line with a negative slope, taken from Fig. 3. These equilibrium states were not attained in the Au capsules for runs at temperatures above 600°C. The relationship between fH_2 and M_{Br^-} is given in Equation (2).

strong influence on the redox states of the fluids in the Au capsules. This is evident from the closeness of the M_{Br^-} values in sensors exposed to fluids inside and outside of the Au capsules for each run; their differences as given in Table 1 are less than 0.2 log unit, even for those runs in which the Co-CoO-H_2O assemblage is protected by double layers of Au (configuration (c) in Fig. 2).

It has been shown previously (CHOU, 1986, his Equation (9)), that the rate of hydrogen transfer across a cylindrical metal membrane at steady state, dM_{H_2}/dt, can be described by

$$dM_{H_2}/dt = [2\pi\kappa l/\ln (r_e/r_i)][|(f^iH_2)^{1/2} - (f^eH_2)^{1/2}|], \quad (6)$$

where κ is permeability constant of the metal membrane to hydrogen, l is the overall length of the cylinder, r_e and r_i are the outer and inner radii of the cylinder, respectively, and f^iH_2 and f^eH_2 are the internal and external hydrogen fugacities of the cylindrical container, respectively. According to Equation (6), there should have been no hydrogen transfer across the inner Au capsule in the double Au capsule experiments (type (c) in Fig. 2) because both sides of the inner membrane are exposed to the same redox buffer and therefore no driving force should exist for the diffusion and permeation of hydrogen (*i.e.*, $(f^iH_2)^{1/2} - (f^eH_2)^{1/2} = 0$). However, this is not the case; the $\Delta H_2O/t$ data given in Table 1 indicate significant hydrogen loss from the inner Au capsule. The rapid outflow of H_2 through the outer Au capsule may generate some finite difference in fH_2 between the internal and external fluids of the inner Au capsule, such that $f^iH_2 > f^eH_2$, even though the two fluid phases were buffered by the same redox buffer assemblage. In Equation (6), equilibrium adsorption and desorption reactions are assumed at the internal or external faces of the membrane, such that

$$1/2\ H_{2(g)} = H_{(membrane)}$$

$$K_s = C_H/(f_{H_2})^{1/2} \quad (g/cm^3\ bar^{1/2}) \quad (7)$$

where K_s is the equilibrium constant for the hydrogen adsorption or desorption and C_H is the hydrogen concentration in the membrane (g/cm^3). It is conceivable that for a given metal at a fixed P-T condition, the K_s value may depend upon the nature of the fluid matrix to which the metal is exposed. For example, because Ar is more inert than H_2O, the desorption constant of hydrogen at the Au/Ar interface may be greater than that at the Au/H_2O interface, such that for a given fH_2 at P and T, $(C_H)^{Au/Ar} > (C_H)^{Au/H_2O}$. Therefore, the permeability constant, κ, derived from Au/H_2O adsorption and desorption interface experiments (CHOU, 1986) cannot be applied to cases where the desorption interface is Au/Ar; κ in the latter should be smaller. Consequently, according to Equation (6), for a given dimension of Au cylinder and a given $|(f^iH_2)^{1/2} - (f^eH_2)^{1/2}|$ value in systems having the same Au/H_2O absorption interface, dM_{H_2}/dt should be higher when the desorption interface is Au/H_2O rather than Au/Ar. In other words, Au is a more efficient hydrogen shield when Ar rather than H_2O is used as an external pressure medium. The apparent similarity in dM_{H_2}/dt values for runs under Ar and H_2O external pressures at the same P-T conditions, as indicated by their similar $|\Delta H_2/t|$ values listed in Table 1, is due to the fact that under Ar pressure, the smaller κ is compensated for by the larger $|(f^iH_2)^{1/2} - (f^eH_2)^{1/2}|$ (see Equation (6) and the fH_2 differences between two sides of Au membrane inferred from the differences in M_{Br^-} between filled and open symbols shown in Figs. 3 and 4).

It can be concluded that in hydrothermal experiments where the Co-CoO-H_2O buffer assemblage is used in the oxygen-buffer technique to control their redox states, equilibrium redox states of the buffer can be obtained in sealed Au capsules of 0.2 mm wall thickness between 500 and 800°C under 2 kbar of either Ar or CH_4 external pressure but cannot be obtained at temperatures between 600 and 800°C under 2 kbar of H_2O external pressure. For more reducing buffers, such as WO_2-WO_{2+x}-H_2O, $Fe_{1-x}O$-Fe_3O_4-H_2O, Fe-Fe_3O_4-H_2O, and Fe-$Fe_{1-x}O$-H_2O, there is no doubt that equilibrium redox states cannot be obtained in Au capsules of 0.2 mm wall thickness, as demonstrated by CYGAN and CHOU (1987) for the WO_2-WO_{2+x}-H_2O buffer under Ar and CH_4 as well as H_2O external pressure. The measured steady-state fH_2's in the Au capsules are much lower than the calculated equilibrium values, mainly due to high rates of H_2 leakage.

KINETICS OF BUFFER REACTIONS

In order to maintain the equilibrium redox states of a buffer system at P and T in the Au capsule shown in Fig. 1, the buffer reaction rate has to be fast enough that the generation or consumption of H_2 in the buffer reaction can effectively counterbalance the loss or gain of H_2 in the system due to H_2 leakage through the outer capsule. The fH_2-sensor measurements for various buffer assemblages in Au capsules under 2 kbar Ar external pressure and between 600 and 800°C made by CHOU (1978) indicate that equilibrium redox states can be maintained for the buffer assemblages MnO-Mn_3O_4-

H_2O, Ni-NiO-H_2O (NNO), and Co-CoO-H_2O. This is demonstrated by the linear relationship shown in Fig. 5 for these buffers, as follows from (1),

$$\log (m_{HCl})_{P,T} = 1/2 \log f H_2 - 1/2 \log K_1. \quad (8)$$

In Fig. 5, the chevrons indicate the reversed sensor HCl measurements for any given buffer. There are a number of chevron pairs for each buffer because different thermodynamic data from literature can be used to calculate the corresponding $f H_2$ value. The sloping line, on the other hand, is based upon the assumption that the NNO point is experimentally and thermodynamically sound, a case argued in CHOU (1978) that for brevity will not be repeated here, with the slope of ½ corresponding to the value given by Equation (8). The circles, then, are the implied correct $f H_2$ values for all other buffers, including MH (magnetite-hematite-H_2O) and FMQ (fayalite-magnetite-quartz-H_2O). It can be argued that point 4 (HAAS and ROBIE, 1973, thermodynamic data) is essentially correct and therefore $f H_2$ equilibrium was attained in our sensor experiment with that buffer. However we feel, on the basis of our own experience with MH, that a somewhat lower $f H_2$ is probably correct and the HCl value given by the sensor was too high. From Equation (8) it is clear that higher HCl would correspond to a higher $f H_2$ value, and, therefore, H_2 leaked *into* the buffer assemblage tube. A similar argument applies to FMQ. In this case, however, point 10 is not based upon thermodynamic calculations; rather, it is an experimental hydrogen membrane measurement, which is apparently near the correct value. The other FMQ points show HCl values that are too low, indicating that H_2 leaked *out* of the buffer assemblage tube.

To minimize the influx of H_2 in the Au capsule containing the MH buffer and to prolong the life span of the buffer, it has been a common laboratory

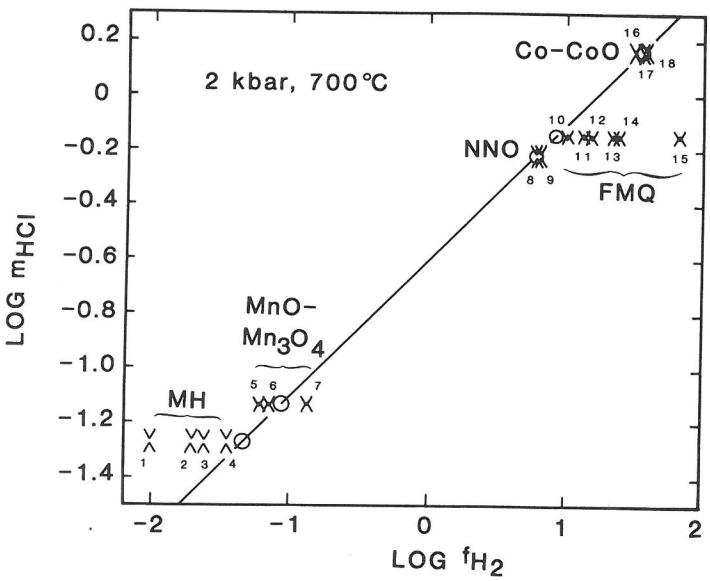

FIG. 5. The internal consistency of $f H_2$ values of various buffers at 2 kbar and 700°C derived from $f H_2$-sensor experiments (open circles) compared with values calculated from various sources of thermodynamic data (chevrons). Values of m_{HCl} are calculated for each of the redox buffers from experimental data of CHOU (1978) as described in CHOU (1987a). One set of m_{HCl} values is given for each buffer (∧ for sensor A and ∨ for sensor B). The $f H_2$ values are calculated from: (1) and (18) ROBIE and WALDBAUM (1968); (2) and (14) EUGSTER and WONES (1962); (3), (15), and (16) SCHWAB and KÜSTNER (1981); (4) HAAS and ROBIE (1973); (5) CHARETTE and FLENGAS (1968); (6) and (9) HAAS (in CHOU, 1987a); (7) and (8) HUEBNER and SATO (1970); (10) MYERS and EUGSTER (1983); (11) HEWITT (1978); (12) O'NEILL (1987); (13) WONES and GILBERT (1969); and (17) MYERS and GUNTER (1979). The dissociation constants for H_2O are taken from ROBIE *et al.* (1979) and the $f H_2O$ data are from BURNHAM *et al.* (1969) in calculating $f H_2$ from $f O_2$ values. The relation between log m_{HCl} and log $f H_2$ given in Equation (8) is shown by the solid line assuming the $f H_2$ values for NNO buffer in (8) is correct; the open circles are located based on this assumption (for detail, see CHOU, 1978). Deviation of the chevrons from the solid line indicates that either the thermodynamic data for other redox buffers are not consistent with the precise NNO buffer data or the measured values for m_{HCl} are not equilibrium values (see text).

practice to use hematite instead of a magnetite-hematite mixture as the initial solid buffer material and CO_2 or Ar instead of H_2O as an external pressure medium. This practice has been quite successful because the use of CO_2 and Ar instead of H_2O lowers the fH_2 gradients across the Au membrane and also possibly lowers Au's permeability constant to hydrogen, as discussed above. However, the assumption that equilibrium redox control of the MH buffer exists in this experimental system is still questionable, as indicated in Fig. 5, even when the buffering material is still far from being exhausted.

The intrinsic fH_2's in Au capsules containing the FMQ-H_2O assemblage were measured under 2 and 4 kbar Ar external pressure and between 600 and 800°C by using the fH_2 sensors (CHOU, 1978). These data are recalculated to 1 kbar pressure in order to compare with other data in the literature, and the results are shown in Fig. 6. It should be emphasized that the fH_2-sensor measurements give the true fH_2 values in the Au capsules as demonstrated by the reversals from sensors A and B (triangles in Fig. 6). However, these fH_2 values are not necessarily the equilibrium values imposed by the buffer because (1) the measured fH_2's are built up by the decomposition of H_2O according to the reaction

$$3\ Fe_2SiO_{4(s)} + 2\ H_2O = 2\ Fe_3O_{4(s)} + 3\ SiO_{2(s)} + 2\ H_{2(g)}, \quad (9)$$

and the reversal of this buffer reaction has not yet been demonstrated, and (2) H_2 may have leaked out of the buffer system. Consequently, the measured fH_2's would tend to be lower than the equilibrium values. For example, the fH_2-sensor measurements indicate that the fH_2 generated by reaction (9) in a sealed Au capsule at 1 kbar and 700°C is about 5.5 bars. This value is lower than the equilibrium value of 6.8 bars derived from the data of MYERS and EUGSTER (1983), indicating that only about 80% of the equilibrium fH_2 value can be achieved. If HEWITT's (1978) equilibrium fH_2 value of 8.4 bars is adopted, then the fH_2 generated in the Au capsule is only about 65% of the equilibrium value. In other words, if the FMQ-H_2O assemblage is used as a hydrogen source in the redox experiment, H_2 generation will be sluggish and the equilibrium fH_2's will be difficult to obtain even when there is no H_2 leakage from the Au capsule. Similarly, our preliminary data indicate that the H_2 consumption reaction of the FMQ buffer (Equation (9) to the left) is even more sluggish, and the fH_2 in the system has to be considerably higher than

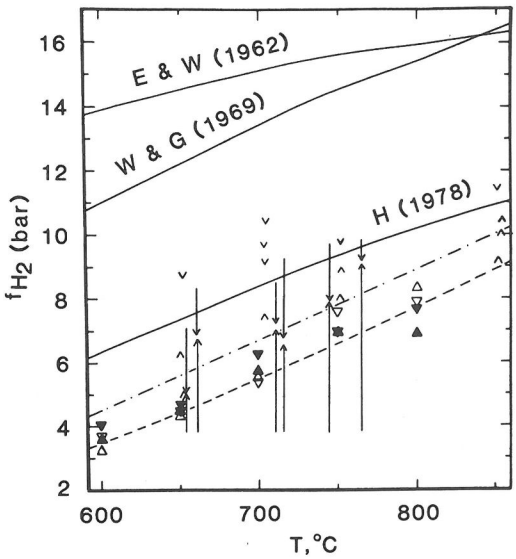

FIG. 6. Comparison of experimental reversals for the buffer assemblage Fe_2SiO_4-Fe_3O_4-SiO_2-H_2O (FMQ) at 1 kbar. Data of HEWITT (1978) are shown by chevrons and those of MYERS and EUGSTER (1983) by arrows, the two ends of arrows indicating the initial and final fH_2. Dash-dot line is a regression of MYERS and EUGSTER's data. Open and solid triangles are calculated, respectively, from 2- and 4-kbar data of CHOU (1978); right-side-up triangles are from sensor A and the inverted triangles are from sensor B. The reversals shown by the triangles indicate the attainment of osmotic equilibrium among the fH_2 sensors and the FMQ buffer system in the experiments and do not demonstrate reversals of the buffer reaction. The dashed curve is the least-squares fit of Chou's data. Solid curves are for EUGSTER and WONES (1962), WONES and GILBERT (1969), and HEWITT (1978).

the equilibrium value to drive the reaction. Erroneous interpretations may result from the invalid assumption that equilibrium redox control by the FMQ buffer in the experimental system has been achieved simply from the post-experiment observation that the buffer assemblage has not been exhausted. We should recognize the fact that at a fixed *P-T* condition, the assemblage FMQ-H_2O does not fix fH_2 in the experimental system at its equilibrium value. In an experimental system, the univariant curve defined by the FMQ buffer in an isobaric fO_2-*T* space is not a thin line but rather a wide band.

It is equally important to recognize the fact that the fH_2 level generated in a sealed Au capsule in hydrothermal experiments by the decomposition of H_2O in certain buffer assemblages depends not only on the nature of the buffer reaction but also on the ratio of H_2O to the solid buffer. For example, the fH_2-sensor measurements for the Ni-NiO-H_2O buffer at 2 kbar and 600°C are given in Table 2 for

Table 2. The effect of H_2O/Ni ratio on the fH_2 values generated in 44 hours by the assemblage Ni-NiO-H_2O contained in Au capsules of 0.2 mm wall thickness at 2 kbar Ar external pressure and 600°C

Run no.	H_2O (mg)	Ni (mg)	NiO (mg)	M_{Cl^-} [a] (±0.005)	fH_2 (bar)
RR 5	17.7	196.2	197.0	0.400; (0.394)	4.2 [b]
RR 3	19.0	62.9	8.6	0.318; (0.321)	2.8 [c]

[a] Measured at 1 atm. and 25°C for the fH_2 sensors containing Ag-AgCl-H_2O-HCl; the numbers in parentheses are from sensors using 3m HCl as a starting solution and the rest are from sensors using H_2O as a starting solution.

[b] The equilibrium value given in Table 3.6 in CHOU (1987a) for run no. BC-76 of 4-day duration at 2 kbar and 600°C; the equilibrium M_{Cl^-} for BC-76 are 0.3899 and (0.3882), which are very close to those given above for RR 5.

[c] Calculated from Equations (3.23) and (3.26) in CHOU (1987a); S and R in Equation (3.26) represent RR 3 and BC-76, respectively.

two runs; one (RR5) has an H_2O/Ni weight ratio of 0.090, and the other (RR3) 0.302, but both have about the same mass of H_2O. After 44 hours, M_{Cl^-} values of fH_2 sensors of RR3 are smaller than the equilibrium value. Assuming the equilibrium fH_2 at 2 kbar and 600°C for the Ni-NiO-H_2O assemblage is 4.2 bars (see CHOU, 1987a, his Table 3.6), then according to Equation (1) the fH_2 in RR3 is 2.8 bars, which is only 66% of the equilibrium value. It is evident from this example that when the surface area of the reactant (Ni in this case) exposed to the H_2O-rich fluid is limited, as in RR3, it will take longer to establish the equilibrium fH_2, if it can be attained at all. Again, the assumption of equilibrium redox control of a buffer system where the ratio of H_2O to solid buffer is high may result in erroneous interpretation of experimental data. The negative deviation of H_2O activity from ideality in H_2O-rich CO_2-H_2O fluids reported by CHOU and WILLIAMS (1979) is an example. We believe that equilibrium fH_2's in the H_2O-rich CO_2-H_2O fluids in that study were not established because of the high ratio of H_2O to the solid buffer in these runs.

COMMENTS ON ANNITE-SANIDINE-MAGNETITE EQUILIBRIUM

The reaction

$$\underset{\text{annite}}{KFe_3AlSi_3O_{10}(OH)_{2(s)}} = \underset{\text{sanidine}}{KAlSi_3O_{8(s)}} + \underset{\text{magnetite}}{Fe_3O_{4(s)}} + H_{2(g)} \quad (10)$$

was the first redox reaction investigated by EUGSTER and WONES (1962) using the oxygen buffer technique. Later, the same reaction was studied by RUTHERFORD (1969), WONES *et al.* (1971), and HEWITT and WONES (1981). These experimental data have been discussed by HEWITT and WONES (1984) and CHOU (1987a). The experimental difficulties described above for the oxygen buffer technique lead to additional comments.

If the solids in Equation (10) are pure,

$$\log K_{10} = \log fH_2. \quad (11)$$

This equilibrium constant as a function of T is shown in Fig. 7 by the two heavy straight lines; one from EUGSTER and WONES (1962)

$$\log fH_2 = (-9215/T, K) + 10.99, \quad (12)$$

and the other from HEWITT and WONES (1984)

$$\log fH_2 = (-8113/T, K) + 9.59 + 0.0042(P - 1)/T, K. \quad (13)$$

It is important to note that the position of Equation (12) is entirely dependent upon the assumption of redox buffer equilibrium, whereas (13) is partially fixed by Shaw membrane experiments at approximately 750°C. The large discrepancy between these two lines, particularly at high fH_2, can be attributed to problems related to redox buffer control. For example, the reversal of reaction (10) observed by EUGSTER and WONES (1962) at 2070 bars along $Fe_{1-x}O$-Fe_3O_4-H_2O (WM) buffer is at 825 ± 5°C and fH_2 = 347 bars, while the fH_2 predicted by Equation (13) at the same P-T condition is only 153 bars, a much lower value than the fH_2 buffered by the WM. Similarly, the reversal observed by EUGSTER and WONES (1962) at 1035 bars along the same buffer is at 785 ± 5°C and fH_2 = 221 bars, while Equation (13) predicts fH_2 = 80 bars. These large discrepancies can be explained if the fH_2 values actually obtained by EUGSTER and WONES (1962) in their Au capsules pressurized externally by H_2O at various P-T conditions were much less than their corresponding equilibrium values defined by the WM buffer, similar to our observations for the Co-CoO-H_2O buffer (Fig. 4) and for the WO_2-WO_{2+x}-H_2O assemblage (CYGAN and CHOU, 1987).

The reversal of reaction (10) reported by RUTHERFORD (1969) along the C-CH_4 buffer is at 830 ± 5°C and fH_2 = 306 bars, which is calculated from thermochemical data assuming equilibrium redox control of the buffer (EUGSTER and SKIPPEN, 1967). As shown in Fig. 7, this data point essentially agrees with the reversal point obtained along the WM buffer at 2070 bars by EUGSTER and WONES (1962).

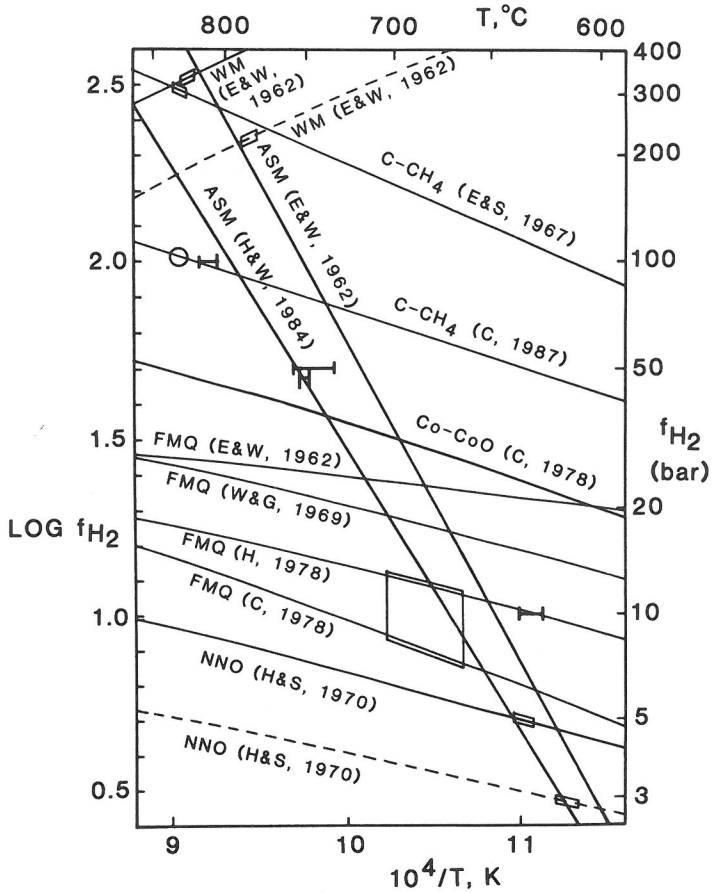

FIG. 7. Summary of experimental results for the reaction annite = sanidine + magnetite + H_2 (reaction 10). The light solid and dashed lines are buffer curves at 2 and 1 kbar, total pressure, respectively. The parallelograms are reversals for reaction (10) based on the data of EUGSTER (1959; on FMQ buffer) EUGSTER and WONES (1962; on WM, FMQ, and NNO buffers), and RUTHERFORD (1969; on C-CH_4 and FMQ buffers). Note that the parallelograms on FMQ and NNO buffers have been shifted from their original positions because of the use of more reliable buffer calibration curves. The open circle represents Rutherford's reversal on C-CH_4 buffer using the calibrated buffer curve (CHOU, 1987b) instead of the calculated one (EUGSTER and SKIPPEN, 1967). The data sources for FMQ buffer are given in Fig. 6. The Co-CoO-H_2O buffer (CHOU, 1978) is shown here for reference. The horizontal bars are reversal data for reactions (10) obtained by the Shaw bomb technique; those at 10, 50 and 100 bars fH_2 are from WONES *et al.* (1971), and the one at 47 bars is from HEWITT and WONES (1981). The two heavy lines marked ASM represent the equilibrium constant for reaction (10) given by EUGSTER and WONES (1962) (Equation 12) and HEWITT and WONES (1984) (Equation 13). For the explanation of the discrepancies between these two lines, see text.

However, the real fH_2 values determined by using the C-CH_4 buffer are much lower than the equilibrium values (CHOU, 1987b, also shown in Fig. 7). Therefore, the reversal point observed by Rutherford (1969) at 2 kbar and 830°C along the C-CH_4 buffer should be at $fH_2 \approx 100$ bars (open circle in Fig. 7) instead of 306 bars. The value is approximate because the C-CH_4 buffer calibration is system specific, although it may be applied in a general way to the experimental system used by RUTHERFORD (1969). This new reversal point agrees fairly well, as shown in Fig. 7, with the reversal point observed by WONES *et al.* (1971) at 1 kbar and 812 ± 6°C with fH_2 = 100 bars. Note that the reversal point at 1 kbar, 746 ± 12°C and fH_2 = 50 bars observed by WONES *et al.* (1971) also agrees well with the point obtained by using the improved Shaw bomb technique at 1 kbar, 752 ± 3°C and fH_2 = 47 ± 3 bars (HEWITT and WONES, 1981; also see Fig. 7). However, the reversal point observed by WONES *et al.* (1971) at 1 kbar, 631 ± 6°C and fH_2 = 10 bars does not agree with the reversal points defined by

observations along the Ni-NiO-H_2O buffer at 2070 bars and 635 ± 5°C and at 1050 bars and 615 ± 5°C (EUGSTER and WONES, 1962; also see Fig. 7). This is probably due to the inadequacy of the Shaw bomb technique in low fH_2 experiments. On the other hand, at these P-T-fH_2 conditions the use of the Ni-NiO-H_2O buffer is ideal because the hydrogen leakage and the slow kinetics of the buffer reaction problems described previously are minimal to non-existent. We agree with HEWITT and WONES (1984) that the original reversed points along the Ni-NiO-H_2O buffer (EUGSTER and WONES, 1962) should be adopted.

The relatively large reversal brackets, in terms of both T and fH_2, for reaction (10) along the FMQ buffer, as shown in Fig. 7, reflect the inadequacy of using the FMQ-H_2O assemblage as a buffer as described previously. Similarly, the reversal point along the MH-H_2O buffer at 2 kbar and 440 ± 5°C, (HEWITT and WONES, 1981), not shown on Fig. 7, needs to be verified. Our initial experiments using fH_2 sensors have been unable to verify this reversal point.

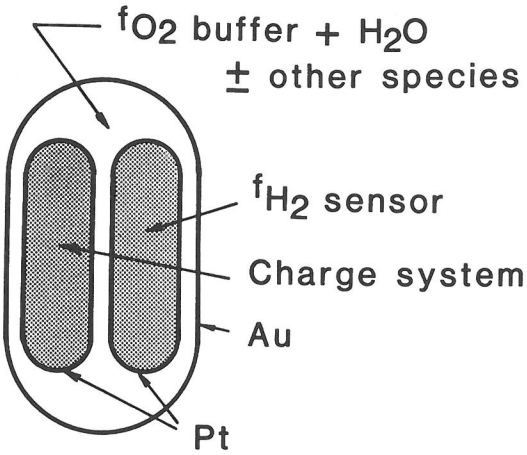

FIG. 8. Schematic diagram showing experimental arrangement for quantitative redox control and measurement. The other species commonly used to reduce fH_2O in the buffer system are salts or stable gases produced by decomposition of $Ag_2C_2O_4$ or AgN_3. Alternately, the charge system and the fH_2 sensor can be exposed directly to the external pressure medium, the fH_2 of which is controlled semiquantitatively (see text).

QUANTITATIVE REDOX CONTROL

Direct fH_2-sensor measurements as well as the experimental data on annite-sanidine-magnetite equilibrium described above demonstrate that equilibrium redox conditions may not always be obtained for buffer assemblages in hydrothermal experimental systems using the oxygen-buffer technique of EUGSTER (1957). This is especially true when H_2O is used as an external pressure medium and the redox conditions of the system are more oxidizing than those defined by the MnO-Mn_3O_4-H_2O buffer or more reducing than those defined by the FMQ-H_2O buffer. The presence of the buffering phases examined after quench is a necessary condition but not sufficient proof for equilibrium redox control during the run. Therefore it is necessary to incorporate an fH_2 sensor into the experiment design (Fig. 8) to monitor the true redox conditions. Even though continuous monitoring of redox conditions during the run is not practical, deviations from equilibrium redox conditions can be detected and subsequent erroneous assumptions of equilibrium redox control can be avoided. Furthermore, since the exact redox condition of the experimental system will be determined by the fH_2 sensor, several semiquantitative redox control methods can be adopted such that intentional deviations from redox conditions defined by the conventional solid-oxygen buffers can be achieved. For example, the charge system and the fH_2 sensor shown in Fig. 8 can be exposed directly to the pressure medium in the pressure vessel and the fH_2 of the system can be controlled semiquantitatively by using various pressure media such as H_2O, CO_2, Ar, CH_4, and mixtures of Ar and H_2 (SHAW, 1963) or Ar and CH_4 (POPP *et al.*, 1984). Alternatively, the fH_2 values buffered by the external system shown in Fig. 8 can be lowered by lowering fH_2O through the addition of a second species in the vapor phase of the external system (WHITNEY, 1972). Silver oxalate ($Ag_2C_2O_4$) and silver azide (AgN_3; KEPPLER, 1989) are convenient sources for CO_2 and N_2, respectively, to be used for this purpose. Salts such as NaCl (FRANZ, 1982) and KCl can also be used. However, it should be kept in mind that unless the fluid at P and T is saturated with respect to the salt added, the fH_2 in the experimental system is only semiquantitatively controlled instead of being defined or buffered, because the system is open to H_2O and therefore its fH_2O and fH_2 are not rigorously defined. Fortunately, since the quantities of H_2O in the system before and after the run can easily be determined gravimetrically, the overall changes in fH_2O and fH_2 in the run can be determined, and these changes can be reduced by minimizing the hydrogen fluxes across the inner and outer capsule walls. To determine the reaction direction in the charge system shown in Fig. 8, monitoring the gain or loss of H_2O in the charge system may be more sensitive than the conventional methods based upon analysis of the solid reaction products. This ap-

proach, together with the quantitative redox control methods described above, has been successfully applied to the studies of mineral stability relations in the skarn system Ca-Fe-Si-O-H (MOECHER and CHOU, 1989).

CONCLUSIONS

Direct fH_2-sensor measurements in hydrothermal experimental systems using the oxygen-buffer technique of EUGSTER (1957) indicate that equilibrium redox conditions may not have been achieved and maintained at the run conditions. This is primarily due to the slow kinetics of the buffer reactions and/or the significant hydrogen leakage through the container of the system, particularly when H_2O instead of Ar is used as an external pressure medium and when the redox states of the system are quite different from those of the pressure medium. The inconsistent experimental data reported by various investigators for the annite-sanidine-magnetite-vapor equilibria, for example, can be explained by the invalid assumption of equilibrium redox control in some of the experiments. The incorporation of an fH_2 sensor in each redox-related experiment can ensure that proper redox control in the experiments using the conventional oxygen buffers has been achieved. It also provides a way to control and measure deviations of the redox states from those defined by these buffers.

Acknowledgements—I-Ming Chou had the privilege of working closely with Prof. Hans P. Eugster for about six years at The Johns Hopkins University, first as a graduate student and later as a postdoctoral fellow and a research associate. Without Hans' pioneering work on the solid-oxygen buffers and his constant guidance and encouragement, this contribution would not have been possible. J. S. Huebner kindly provided access to his high-pressure equipment and X-ray facilities. Reviews by H. T. Haselton, J. J. Hemley, W. D. Gunter, and G. B. Skippen were greatly appreciated.

REFERENCES

BURNHAM C. W., HOLLOWAY J. R. and DAVIS N. P. (1969) Thermodynamic properties of water to 1000°C and 10,000 bars. *Geol. Soc. Amer. Special Paper* **132**, 96pp.

CHARETTE G. G. and FLENGAS S. N. (1968) Thermodynamic properties of the oxides of Fe, Ni, Pb, Cu, and Mn by EMF measurements. *J. Electrochem. Soc.* **115**, 796–804.

CHOU I-MING (1978) Calibration of oxygen buffers at elevated P and T using the hydrogen fugacity sensor. *Amer. Mineral.* **63**, 690–703.

CHOU I-MING (1986) Permeability of precious metals to hydrogen at 2 kb total pressure and elevated temperatures. *Amer. J. Sci.* **286**, 638–658.

CHOU I-MING (1987a) Oxygen buffer and hydrogen sensor techniques at elevated pressures and temperatures. In *Hydrothermal Experimental Techniques* (eds. G. C. ULMER and H. L. BARNES), pp. 61–99. J. Wiley & Sons, New York.

CHOU I-MING (1987b) Calibration of the graphite-methane buffer using the fH_2 sensors at 2 kilobar pressure. *Amer. Mineral.* **72**, 76–81.

CHOU I-MING (1988) Quantitative redox control in hydrothermal experiments (abstr.) *EOS* **69**, 528.

CHOU I-MING (1989) A low-temperature redox sensor (abstr.) *EOS* **70**, 507.

CHOU I-MING and CYGAN G. L. (1987) Effect of pressure medium on redox control in hydrothermal experiments (abstr.). *EOS* **68**, 451.

CHOU I-MING and CYGAN G. L. (1989) Equilibrium and steady-state redox control in hydrothermal experiments (abstr.). *28th Internat. Geol. Congr.* 1–287.

CHOU I-MING and EUGSTER H. P. (1976) A sensor for hydrogen fugacities at elevated P and T and applications (abstr.). *EOS* **57**, 340.

CHOU I-MING and WILLIAMS R. J. (1979) Activity of H_2O in supercritical fluids: H_2O-CO_2 at 600° and 700°C at elevated pressures (abstr.). *Lunar Planet. Sci.*, **X**, 201–203.

CYGAN G. L. and CHOU I-MING (1987) Calibration of the WO_2-WO_3 buffer (abstr.). *EOS* **68**, 451.

EUGSTER H. P. (1957) Heterogeneous reactions involving oxidation and reduction at high pressures and temperature. *J. Chem. Phys.* **26**, 1760–1761.

EUGSTER H. P. and SKIPPEN G. B. (1967) Igneous and metamorphic reactions involving gas equilibria. In *Researches in Geochemistry*, Vol. 2 (ed. P. H. ABELSON), pp. 492–520. Wiley, New York.

EUGSTER H. P. and WONES D. R. (1962) Stability relations of the ferruginous biotite, annite. *J. Petrol.* **3**, 81–124.

FRANZ G. (1982) The brucite-periclase equilibrium at reduced H_2O activities: some information about the system H_2O-NaCl. *Amer. J. Sci.* **282**, 1325–1339.

HAAS J. L., JR. and ROBIE R. A. (1973) Thermodynamic data for wüstite, $Fe_{0.947}O$, magnetite, Fe_3O_4, and hematite, Fe_2O_3. *EOS* **54**, 483.

HEWITT D. A. (1978) A redetermination of the fayalite-magnetite-quartz equilibrium between 650° and 850°C. *Amer. J. Sci.* **278**, 715–724.

HEWITT D. A. and WONES D. R. (1981) The annite-sanidine-magnetite equilibrium (abstr.). GAC-MAC Joint Annual Meeting, Calgary, **6**, A-66.

HEWITT D. A. and WONES D. R. (1984) Experimental phase relations of the micas. In *Mica* (ed. S. W. BAILEY), Reviews of Mineralogy **13**, pp. 201–256. Mineral. Soc. Amer.

HUEBNER J. S. (1971) Buffering techniques for hydrostatic systems at elevated pressures. In *Research Techniques for High Pressure and High Temperature* (ed. G. C. ULMER), pp. 123–177. Springer-Verlag, New York.

HUEBNER J. S. and SATO M. (1970) The oxygen fugacity-temperature relationships of manganese and nickel oxide buffers. *Amer. Mineral.* **55**, 934–952.

KEPPLER H. (1989) A new method for the generation of N_2-containing fluids in high-pressure experiments. *Eur. J. Mineral.* **1**, 135–137.

MOECHER D. P. and CHOU I-MING (1989) Experimental study of equilibria in the system Fe-Ca-Si-O, and revised estimates of $\Delta_f G^0_{298}$ for andradite and hedenbergite (abstr.). *Geol. Soc. Amer. Abstr. with Progr.* **21**, A156.

MYERS J. and EUGSTER H. P. (1983) The system Fe-Si-

O: Oxygen buffer calibrations to 1500K. *Contrib. Mineral. Petrol.* **82,** 75–90.

MYERS J. and GUNTER W. D. (1979) Measurement of the oxygen fugacity of the cobalt-cobalt oxide buffer assemblage. *Amer. Mineral.* **64,** 224–228.

O'NEILL H. ST. C. (1987) Quartz-fayalite-iron and quartz-fayalite-magnetite equilibria and the free energy of formation of fayalite (Fe_2SiO_4) and magnetite (Fe_3O_4). *Amer. Mineral.* **72,** 67–75.

POPP R. K., NAGY K. L. and HAJASH A., JR. (1984) Semi-quantitative control of hydrogen fugacity in rapid-quench hydrothermal vessels. *Amer. Mineral.* **69,** 557–562.

ROBIE R. A. and WALDBAUM D. R. (1968) Thermodynamic properties of minerals and related substances at 298.15K (25°C) and one atmosphere (1.013 bars) pressure and at higher temperatures. *U.S. Geol. Surv. Bull.* **1259,** 256pp.

ROBIE R. A., HEMINGWAY B. and FISHER J. R. (1979) Thermodynamic properties of minerals and related substances at 298.15K and 1 bar (10^5 Pascals) pressure and at higher temperatures. *U.S. Geol. Surv. Bull.* **1452** (Reprint with corrections 1979), 456pp.

RUTHERFORD M. J. (1969) An experimental determination of iron biotite-alkali-feldspar equilibria. *J. Petrol.* **10,** 381–408.

SCHWAB R. G. and KÜSTNER D. (1981) The equilibrium fugacities of important oxygen buffers in technology and petrology. *Neues Jahrb. für Mineral. Abhandl.* **140,** 111–142.

SHAW H. R. (1963) Hydrogen-water vapor mixtures: control of hydrothermal atmospheres by hydrogen osmosis. *Science* **139,** 1220–1222.

WHITNEY J. A. (1972) The effect of reduced H_2O fugacity on the buffering of oxygen fugacity in hydrothermal experiments. *Amer. Mineral.* **57,** 1902–1908.

WONES D. R. and GILBERT M. C. (1969) The fayalite-magnetite-quartz assemblage between 600 and 800°C. *Amer. J. Sci.* **267,** 480–488.

WONES D. R., BURNS R. G. and CARROLL B. M. (1971) Stability and properties of synthetic annite (abstr.). *EOS* **52,** 369.